

Arastırma Makalesi / Research Article

MATHEMATICAL MODEL FOR CALCULATING BREAKING ENERGY OF COMPONENT YARNS IN DUAL-SHEATH SINGLE-CORE HYBRID YARN

Md. Azharul ISLAM^{1,2}
Rochak RATHOUR^{1*}
Bipin KUMAR¹
Apurba DAS¹
Nandan KUMAR³

¹Department of Textile and Fibre Engineering, Indian Institute of Technology Delhi, Hauz Khas, New Delhi, India

²Department of Textile Engineering, Mawlana Bhashani Science and Technology University, Santosh, Bangladesh

³High-Performance Textiles Pvt. Ltd., Panipat, Haryana, India

Gönderilme Tarihi / Received: 17.10.2024

Kabul Tarihi / Accepted: 14.03.2025

ABSTRACT: The increasing utilization of multicomponent hybrid yarns in present world highlights their critical role in advancing protective textile technologies. In this study, hybrid yarns with dual sheath and a single core were produced in varying linear densities and twist directions where polyester and ultra-high molecular weight polyethylene (HPPE) were considered as the sheath components and stainless steel (SS)/glass yarn was taken as core component. The failure pattern and energy required for breakage of hybrid yarn were analyzed, showing that glass-core yarns exhibited multiple cracking tendency, while (SS)-core yarns rarely did. This was attributed to the lower breaking extension % of glass fibers (3.61%-3.81%) compared to SS (18.52%-28.05%), HPPE (5.20%-6.21%), and polyester (17.05%). Glass-core yarns reached their breaking extension earlier, leading to premature breakage. A mathematical model developed from load-extension curves demonstrated that HPPE contributed the most to breaking energy (68.67%), followed by polyester (18.49%) and glass (10.92%). The average absolute error of the model was calculated as 4.87% that led to average ~95% accuracy. The reason for this error was the assumptions about HPPE breakage that were considered during modeling. These findings support researchers in identifying high-performance yarns suitable for cut, stab, and slash-resistant fabrics, ensuring compliance with energy failure standards and allied industrial practices.

Keywords: Composite yarn, core sheath yarn, tensile strength, work of rupture

ÇİFT MANTOLU TEK ÇEKİRDEKLİ HİBRİT İPLİKTE BİLEŞEN İPLİKLERİN KOPMA ENERJİSİNİN HESAPLANMASI İÇİN MATEMATİKSEL MODEL

ÖZ: Çok bileşenli hibrit ipliklerin günümüzde artan kullanımı, koruyucu tekstil teknolojilerinin ilerletilmesindeki kritik rollerini vurgulamaktadır. Bu çalışmada, Çift Mantolu ve tek çekirdekli hibrit iplikler, polyester ve ultra yüksek moleküler ağırlıklı polietilen (HPPE) kılıf bileşenleri, paslanmaz çelik (SS)/cam iplik ise çekirdek bileşeni olarak alınarak farklı doğrusal yoğunluklar ve büküm yönlerinde üretilmiştir. Hibrit ipliklerin kopma paterni ve kopma için gereken enerji analiz edilmiştir; cam çekirdekli ipliklerin çoklu çatlama eğilimi gösterdiği, SS çekirdekli ipliklerin ise nadiren bu durumu sergilediği gözlemlenmiştir. Bu durum, cam liflerinin daha düşük kopma uzaması yüzdesine (%3.61-%3.81) sahip olmasından kaynaklanmaktadır; bu oran SS (%18.52-%28.05), HPPE (%5.20-%6.21) ve polyester (%17.05) liflerinden düşüktür. Cam çekirdekli iplikler, kopma uzamasına daha erken ulaştığından erken kopma meydana gelmiştir. Yük-uzama eğrilerinden geliştirilen matematiksel bir model, HPPE'nin kopma enerjisine en fazla katkısı (%68.67) sağladığını, bunu polyesterin (%18.49) ve camın (%10.92) izlediğini göstermiştir. Modelin ortalama mutlak hatası %4.87 olarak hesaplanmış ve bu, yaklaşık %95 doğruluk sağlamıştır. Bu hata, modelleme sırasında HPPE kopmasıyla ilgili yapılan varsayımlardan kaynaklanmıştır. Bu bulgular, enerji arıza standartları ve ilgili endüstriyel uygulamalara uygunluğu sağlarken, araştırmacılara kesme, delme ve yırtılmaya karşı dayanıklı kumaşlar için yüksek performanslı ipliklerin belirlenmesinde destek sağlamaktadır.

Anahtar Kelimeler: Kompozit iplik, çekirdek kılıf ipliği, çekme dayanımı, kopma işi.

*Sorumlu Yazar/Corresponding Author: india.rochak1994@gmail.com

DOI: <https://doi.org/10.7216/teksmuh.1563481>

www.tekstilmuhendis.org.tr

1. INTRODUCTION

The demand for hybrid high-performance yarn is increasing daily due to its versatility and applications across different industries. They can be used in sectors like automotive [1], aerospace [2], construction [3], protective textiles [4] and others. Its adaptability makes them a valuable component in advanced material applications where specific properties are required. The integration of diverse high-performance materials can significantly improve durability and performance for applications with high demands. When fibers with varying mechanical properties are combined in different configurations to produce hybrid yarns, the potential for multiple cracking under tensile stress becomes apparent. Understanding the conditions that lead to such cracking in both the individual components and the hybrid yarn itself is crucial. This knowledge offers valuable insights for determining the appropriate end-use of the yarn, particularly in sectors such as construction and textile engineering. Moreover, the ability to predict and assess the multiple-cracking behavior of hybrid high-performance yarns can further enhance their durability and functionality in a variety of products, including composites and textile applications [5]. Calculating the energy at break for textile materials, particularly hybrid yarns, is fundamental to enhancing their mechanical performance and durability. The energy at break, which signifies the amount of energy a material can absorb before failing under tensile stress, is directly linked to its toughness and capacity to endure mechanical forces [6]. This measurement is especially critical for high-performance applications, such as protective clothing, where reliability and safety under extreme conditions must be ensured. Despite its importance, little research has focused on measuring and modeling the breaking energy of individual component yarns within hybrid yarns. Most current studies primarily address mechanical properties like tensile strength and elongation, with limited attention paid to the energy at break of hybrid yarns as a whole. This gap highlights the need for further investigation into how the various component yarns influence the energy at which hybrid yarns break, as well as how this can be accurately measured. Comparative studies are also necessary to assess the energy at break of hybrid yarns in relation to traditional fibers. For example, existing research suggests that Bekinox fibers break at approximately 80 N, while hybrid yarns fail at around 70 N, indicating a potentially lower energy at break for hybrid yarns [7].

Additionally, one study demonstrated that the MLI spinning process could enhance the energy at break by 5% compared to the TAJIS process when using stainless steel and polypropylene yarns [8]. In another investigation, Hengstermann and his team developed new hybrid yarns using recycled carbon fibers for use as raw materials in composite production. These recycled carbon fibers were combined with virgin carbon and polyamide 6 to create the final composite, with polyamide 6 exhibiting the highest breaking energy and virgin carbon fiber the lowest [9]. Moreover, to analyze their tensile properties, hybrid yarns were produced from a combination of abaca, mulberry, polyester, and nylon fibers. Researchers primarily focused on stress and strain parameters in these fiber combinations, overlooking the breaking energy of the arrangements [10].

Evaluation of multiple cracking in fibers is widely checked for textile composites. However, there was very limited research on failure behavior of hybrid yarn and no research on energy required to break the individual components used in a hybrid yarn. H. Dalfi et al. showed that hybrid yarns made with alkali-resistant glass and polypropylene exhibit distinct mechanical properties. The differences in tensile strength, elongation, and stiffness among these fibers can lead to differential strain under loading. This discrepancy results in uneven stress distribution within the yarn, initiating cracks, particularly in the more brittle fibers, as they fail to accommodate the deformation experienced by their more ductile counterparts [11]. Multiple cracking sometime occurs in a multiple component yarn when stress on the yarn exceeds certain limits. This cracking can be occurred before reaching the ultimate strength of material used in a composite material [12]. This cracking usually propagates perpendicular to the load application direction [13]. It is also seen in another research that, material properties like breaking elongation and tensile strength of hybrid yarns significantly affects the cracking behavior under tensile loading. Specially, the crystallinity and surface morphology of the component yarns can modify the interaction within the fibers or yarns and consequently contributes in the cracking response [14]. As an example, the presence of load-aligned crimped yarns leads to distinct damage mechanisms, influencing the cracking evolution and opening of textile based composite material [15]. Research shows that as the strain exceeded a critical threshold, multiple cracking modes become evident, reflecting the mechanical behavior of the yarns under different deformation stages [16]. These patterns are typically influenced by factors such as yarn type and arrangement of yarns in the hybrid yarn and its composites, affecting how the tensile strength is distributed and utilized within the component yarns and the matrix that used [3].

Multiple cracking is rarely found in hybrid yarns produced using natural fibers through traditional spun yarn technology. However, in hybrid yarns composed of high-performance fibers, the likelihood of multiple cracking increases. This phenomenon does not occur uniformly across all combinations of component yarns, and its occurrence cannot be guaranteed in every case. When hybrid yarns consist of fibers with varying stiffness, twist in different layers and number of filaments in each layers, packing density of component yarns and strength, the tensile load may not be evenly distributed throughout the yarn. In such cases, one fiber bundle may reach its breaking point earlier, failing before the remaining components, which continue to bear the load. This uneven stress distribution can lead to a series of cracks, resulting in progressive failure as the load increases [14]. Individual component fibers have a noticeable impact on final yarn failure mechanism. By mixing polyester and viscose in different ratios, the final tensile failure was investigated and reported [17]. Yarn was prepared using ring, rotor and air jet spinning method the failure trend was detected. Contribution of polyester fiber was higher in slippage in rotor and air jet spinning whereas in ring yarn the fiber breakage rate was prominent. It meant that spinning technology wise yarn failure behavior changes and affects the final tensile performance. For the same yarn compositions, the

breakage rate of yarn was observed during winding and a mathematical model was suggested to predict the failure trend. With the lowering of polyester percentage the slippage length of fiber was reduced in the yarn breaking zone for both leading and trailing area [18]. However, this failure architecture of natural and synthetic fiber might provide some idea about the breaking phenomena of hybrid yarn made with High performance yarns (HPYs). With a very brittle characteristics, glass fiber jumped to high performance fiber arena with lots of extra ordinary features. Despite having less bending properties, due to high tensile strength, dielectric characteristics, chemically inert properties demand of glass fiber developing globally [19]. Glass fiber linear density from 50-200 Denier multi filament is commercially available now as days. Research showed that glass fiber can protrude outside after wrapping and converting it to fabric [20]. That is why, it is highly recommended to wrap the glass yarn in such a way that glass fiber will not be able to extrude even after breaking inside and remain there. For this reason, multiple sheath layer is required [21]. In modern era of research, yarns are being made from carbon nanotubes (CNTs) and tensile performance evaluated comparatively higher gauge length of 110 mm [22]. Lager cross sectional area of CNTs yarn showed higher tensile strength than higher densified yarn. It concluded that fiber arrangement promoted the tensile strength over its density. Results also suggested that CNTs needed to study far because of having higher brittle characteristics. It showed less mechanical strength and modulus than commercially produced carbon fibers. Finally, multiple cracking in multicomponent yarns of hybrid yarns occurs during tensile loading, particularly influenced by the yarn arrangement, material properties, and loading conditions. As load is applied, the behavior of component yarns determines the cracking patterns and the mechanical responses of the hybrid yarn.

From the above discussion, it was seen that researchers hardly focused on the individual yarn breaking pattern of a hybrid yarn, and to our best knowledge, energy consumption of individual component yarns of hybrid yarn during break has not been studied yet. For this reason, the final objective of this project was settled as a follow-up on the breaking pattern of individual components of hybrid yarn and made a model to calculate the breaking energy of individual component yarns. As the conventional method does not provide the option to measure individual breaking energy measurements, this research hypothetically focuses on a mathematical model that can measure individual component yarn's breaking energy, and validation will be performed to measure the accuracy percentage of the model. To do that, different layers of hybrid yarn were selected, like SS/glass yarn in the core, HPPE in the outer layer, and polyester yarn in the inner layer to provide cohesion between the core and outer layer.

2. EXPERIMENTAL SETUP

2.1 Yarn preparation

Hybrid yarn can be produced using multiple techniques, such as DREF spinning [23], commingling [24,25], wrap spinning [26] and so on. The spinning technique is chosen depending on the type of raw materials and the tentative final performance of the yarn.

The wrap spinning technique was implemented for this hybrid yarn, where core yarn was covered with polyester and HPPE yarn. Polyester was taken as the inner layer, and HPPE yarn was chosen as the outer layer of the hybrid yarn.

Four distinct types of yarn were selected to produce hybrid high-performance yarn. Given that the focus of this hybrid yarn was to enhance cut and slash resistance in fabrics, glass and stainless steel (SS) were chosen as the core yarns. The polyester yarn was selected for the inner layer of the hybrid yarn. Due to the highly slippery nature of SS, glass, and high-performance polyethylene (HPPE) yarns, maintaining cohesion during the yarn formation process proved challenging. For this reason, an inner layer was necessary to enhance the cohesion between the core and outer layers. Textured polyester yarn, having a higher frictional coefficient than SS, glass, and HPPE, was ideal for holding the core and outer layers together.

SS, HPPE, Glass filament yarns are very costly and keeping the project cost in consideration, the linear density of core and outer sheath layer yarn were increased in same ratio so that the effect of each component yarn remain nearly in same pattern. A total of twelve samples were prepared and divided into two groups. In the first group, SS yarn was used as the core (Figure 1(a)), while glass yarn was utilized in the second group (Figure 1(b)). Both groups featured two outer wrap layers, with polyester as the inner layer and HPPE as the outer layer. Additionally, each group was further divided into two parts based on the twist direction of the inner and outer layers. In three of the samples from each group, both the inner and outer layers were twisted in the same (S) direction, while the remaining three samples had an inner layer twisted in the S direction and an outer layer in the Z direction. In Table 1, the sample formation with selected parameters is presented. Every hybrid yarns were coded as Y1, Y2, Y3.....Y12 where first six samples (Y1 to Y6) consisted of SS yarn in core and last six samples (Y-7 to Y-12) were from glass yarns in core.

Linear density of glass yarn, polyester, and HPPE were selected as available on the market. It was also found in previous works that for wearable textiles in composite or hybrid yarns, below-mentioned yarn density was used by manufacturers with their number of filaments. All the SS yarns were monofilaments having 30, 40, and 50 micron diameters.

2.2 Tensile strength tester

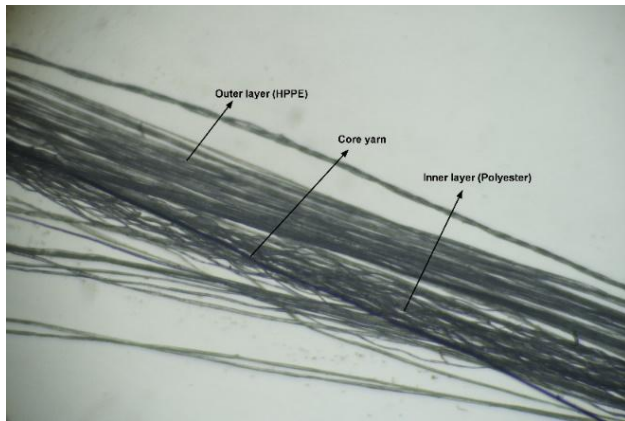
Tensile strength of the yarns were tested using Instron 3365, USA universal strength tester. The calibration action was taken before performing the test. Meanwhile, suitable jaw and load cell were installed and checked with standard parameters. In brief, the gauge length of the machine was set to 250mm, and the extension rate was taken as 300 mm per minute, according to the standard. Fixing test specimen at jaw is a crucial matter for which unwanted multiple cracking graph can be obtained. As it is known that Multiple cracking of yarn can happen either for slippage of yarn in jaw or breaking of yarn components in different times. In this research, to avoid slippage of the yarn, both ends of the testing

yarn specimen were wrapped over the angular jaw ten times. This method prevented the total slippage. The tensile performance of

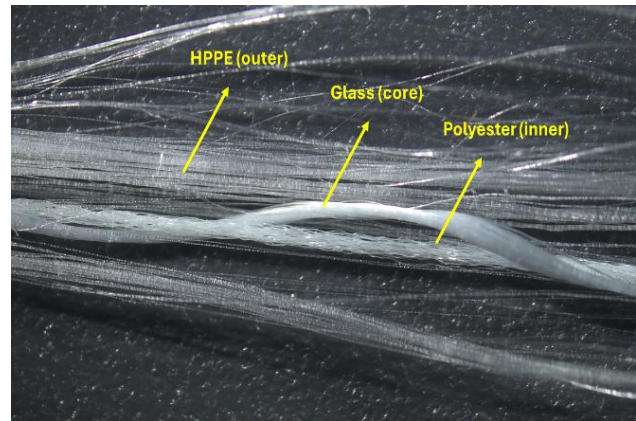
the component yarns were calculated following same method and procedure.

Table 1. Hybrid high-performance yarn with different parameters

Code	Fiber composition			Twist per meter	Twist direction	Calculated final count (Tex)
	SS/Glass (Core)	Polyester (inner layer)	HPPE (outer layer)			
Y1	SS-30	100D	200D	400	S-Z	40
Y2	SS-40		300D		S-Z	65
Y3	SS-50		400D		S-Z	75
Y4	SS-30		200D		S-S	40
Y5	SS-40		300D		S-S	65
Y6	SS-50		400D		S-S	75
Y7	Glass-100D		200D		S-Z	50
Y8	Glass-200D		300D		S-Z	75
Y9	Glass-300D		400D		S-Z	95
Y10	Glass-100D		200D		S-S	50
Y11	Glass-200D		300D		S-S	75
Y12	Glass-300D		400D		S-S	95



(a)



(b)

Figure 1. Three different layers of hybrid high-performance yarn: (a) SS core yarn, (b) Glass core yarn

Table 2. Number of filaments and average diameter of individual fibers of component yarns

Component yarn	Linear density (Den)	Average diameter of individual fiber (µm)	Number of filaments
HPPE	200	20	90
HPPE	300	30	90
HPPE	400	20	180
Glass	100	5.5	200
Glass	200	5.5	400
Glass	300	9.5	200
Polyester	100	20	36

2.3 Fiber morphology

The fiber morphology of the yarns were checked using LEICA DM 2700M, Germany, optical microscope. Lens and slides were examined carefully to confirm their cleanliness. For accurate image, calibration and checking the machine essentials are very important. An integrated software allied with LEICA DM 2700M was used to take the images. For evaluating the diameter and surface of SS, glass, polyester, and HPPE fiber, every kind of fiber was separated and collected on a slide with the help of scotch tape. The purpose of this imaging was to see the diameter variation of the component fibers which may lead to multiple cracking in the final yarn.

2.4 Data analytical tool

The cracking points observed on the load-elongation curve were identified using the annotation tool in Origin 2020b. The key advantage of this tool is its ability to display precise values at any position along the load-elongation curve. By using this tool, the load and elongation values corresponding to each individual cracked component yarn can be recorded, which is essential for further analysis in measuring their breaking energy.

2.5 Multiple cracking phenomenon

Figure 2 shows the multiple cracking that might take place when a product is made of two or more than two different types of components where each of the components bears different tensile properties such as tensile strength, breaking extension, tensile modulus, and so on. This kind of failure characteristics of a material could be found in composite materials or hybrid yarns where different types of materials are accumulated together for different purposes. The first component breaks for having lower breaking extension and breaking strength, and after failing, it can only carry the frictional load, and the load drops immediately after that failure. The rest of the components carries forward the rest of the load remain safe and unbroken [27]. This procedure continues

$$\text{Area of trapeziod} = \frac{1}{2} (\text{summation of length of parallel base}) \times \text{height} \tag{3}$$

till the entire material finally breaks down and completely separates.

2.6 Energy at break calculation

Energy at break of any material can be calculated from load elongation curve achieved from tensile testing. The energy at the break is defined as the area under the curve that is obtained from load elongation graphical presentation. By integrating the equation that follows the curve with the lower and upper limit, it is an extension.

$$\text{Energy at break} = \int_0^{\text{breaking extension}} y dx \tag{1}$$

Where, $y = \text{intercept} + \sum B_i x^i (i = 1,2,3, \dots)$

Here, $y =$ dependent variable, $\text{intercept} =$ value of y when all independent variables are zero, $B_i =$ coefficient of corresponding x_i and $x_i =$ independent variable.

Equation (1) is generally used to calculate the area under the curve, equivalent to energy at break from the load elongation curve of a material. Getting equations from the load elongation curve is essential for energy evaluation and the performance of integration calculations. However, getting the equation is often more complicated when multiple cracking occurs in the sample. This research has suggested another simple mathematical model to overcome the issue. The area under the curve for energy calculation is possible to measure following equation 2, equation 3, and Figure 3. The multiple cracking behavior of the yarn can be segmented into multiple parts, like triangles and trapezoids. The area of each portion can be calculated following the area measurement equations of triangle and trapezoid (equation 2 and equation 3).

$$\text{Area of triangle} = \frac{1}{2} \times \text{base} \times \text{height} \tag{2}$$

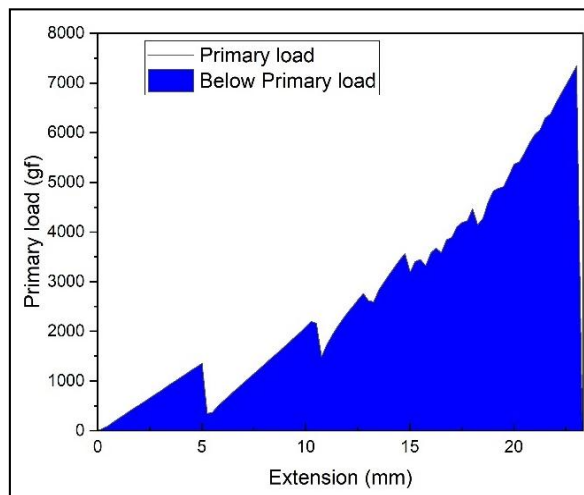


Figure 2. Energy at break behavior of multiple crack yarn

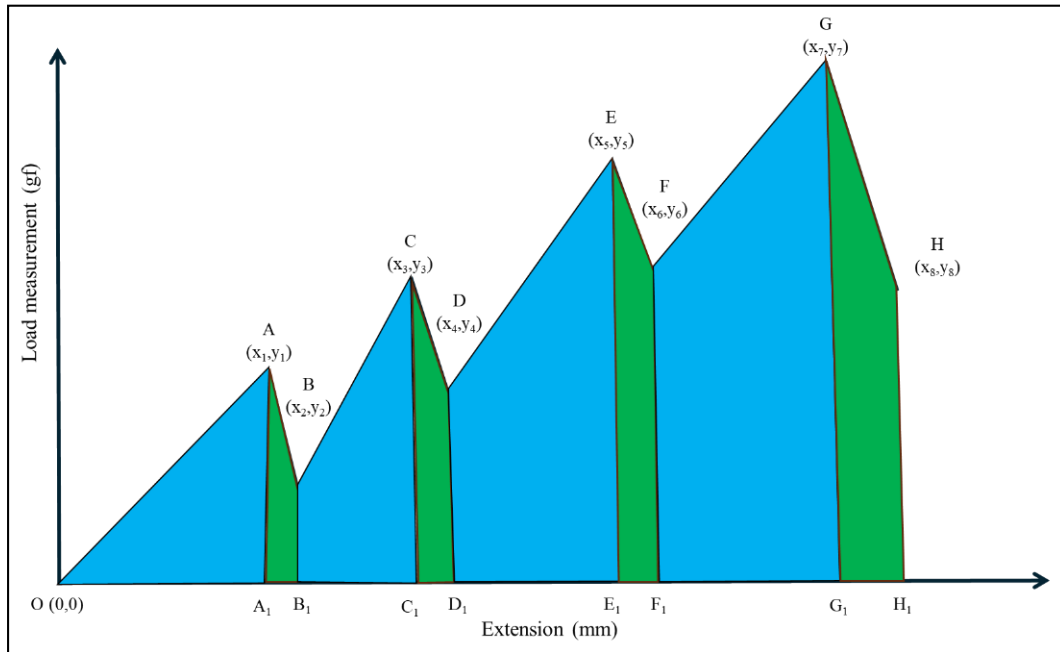


Figure 3. Energy at break evaluation using triangle and trapezoid area calculation method

In Figure 3, point A(x₁,y₁), C(x₃,y₃), E(x₅,y₅) and G(x₇,y₇) represent the failure point of the first, second, third and fourth component yarn within the hybrid yarn structure.

Therefore, following equation 2 and 3, area under the curve (breaking energy) of Figure 3 can be calculated following equation.

$$\begin{aligned}
 \text{Total area} &= \text{area of triangle } OAA_1 + \text{area of trapezoids } (A_1ABB_1 + B_1BCC_1 + C_1CDD_1 + D_1DEE_1 + E_1EFF_1 + F_1FGG_1 + \\
 &G_1GHH_1) = \frac{1}{2}x_1 \times y_1 + \frac{1}{2}(y_1 + y_2)(x_2 - x_1) + \frac{1}{2}(y_2 + y_3)(x_3 - x_2) + \dots + \frac{1}{2}(y_7 + y_8)(x_8 - x_7) = \frac{1}{2}x_1 \times y_1 + \\
 &\frac{1}{2}\sum_{i=1}^n (y_i + y_{i+1})(x_{i+1} - x_i) \tag{4}
 \end{aligned}$$

So, the total energy required to break the yarn will be equivalent to equation (4). From this equation, it is possible to find out the breaking energy of every component yarn following the below equations:

$$\text{Energy required for first component} = \frac{1}{2}x_1 \times y_1 \tag{5}$$

$$\begin{aligned}
 &\text{Energy required for second component} = \text{Energy required for first and second component yarn} - \\
 &\text{Energy required for first component yarn} = \left[\frac{1}{2}x_1 \times y_1 + \frac{1}{2}\sum_{i=1}^3 (y_i + y_{i+1})(x_{i+1} - x_i) \right] - \frac{1}{2}x_1 \times y_1 \tag{6}
 \end{aligned}$$

$$\begin{aligned}
 &\text{Energy required for third component} = \text{Energy required for first, second and third component yarn} - \\
 &\text{Energy required for first and second component yarn} = \left[\frac{1}{2}x_1 \times y_1 + \frac{1}{2}\sum_{i=1}^5 (y_i + y_{i+1})(x_{i+1} - x_i) \right] - \\
 &\left\{ \frac{1}{2}x_1 \times y_1 + \frac{1}{2}\sum_{i=1}^3 (y_i + y_{i+1})(x_{i+1} - x_i) \right\} - \frac{1}{2}x_1 \times y_1 \tag{7}
 \end{aligned}$$

2.7 Assumptions and validation

One key assumption was considered regarding the multiple breaking behavior of HPPE while measuring the breaking energy. For the purpose of predicting the final energy at break, HPPE was

treated as a non-multiple-breaking yarn in the analysis. In Figure 4, the AB line represents the assumed propagation of the curve, based on HPPE’s tensile strength rather than accounting for its multiple cracking tendencies. It is important to note that Figure 4 is derived from the tensile performance of the Y12 glass-core

hybrid yarn, reflecting this assumption in its interpretation. This assumption will deviate from the actual breaking energy and therefore, the validation of the model will be attempted with the actual breaking energy and calculated breaking energy of entire yarn. The deviation between two breaking energies will be signified as absolute error of the model.

3. RESULTS

3.1 Tensile strength of hybrid yarns

Figure 5 presents the tensile behavior of hybrid yarns with stainless steel (SS) cores. In most cases, hybrid yarns with SS cores exhibited single-crack failure modes during collapse. For yarns Y1, Y2, and Y3, which feature an S-Z twist configuration between the inner polyester layer and the outer high-performance polyethylene (HPPE) layer, no multiple cracking was observed

with increasing linear density. However, a tendency toward multiple cracking was noted in the S-S twist configuration of the same yarns, particularly in SS-core hybrid yarns with higher linear densities. The variation in breaking extension was minimal for yarns with lower linear densities, leading to single-crack failure. In contrast, in yarns with higher linear densities, SS tended to fail first, followed by the simultaneous failure of polyester and HPPE.

Figure 6 illustrates the tensile performance of hybrid yarns with glass cores. The samples Y7 to Y9, featuring an S-Z twist direction for both the inner and outer layers, are displayed at the top, while samples Y10 to Y12, which have an S-S twist configuration for the same layers, are shown at the bottom. The S-S twisted yarns exhibited a higher tendency for multiple cracking compared to the S-Z twisted yarns. However, multiple cracking was also observed in the S-Z twisted yarns, though it occurred less frequently than in the S-S twisted yarns.

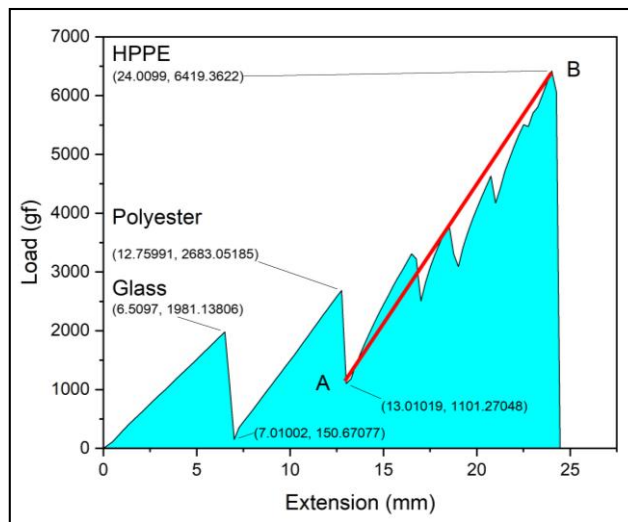


Figure 4. HPPE yarn cracking assumption

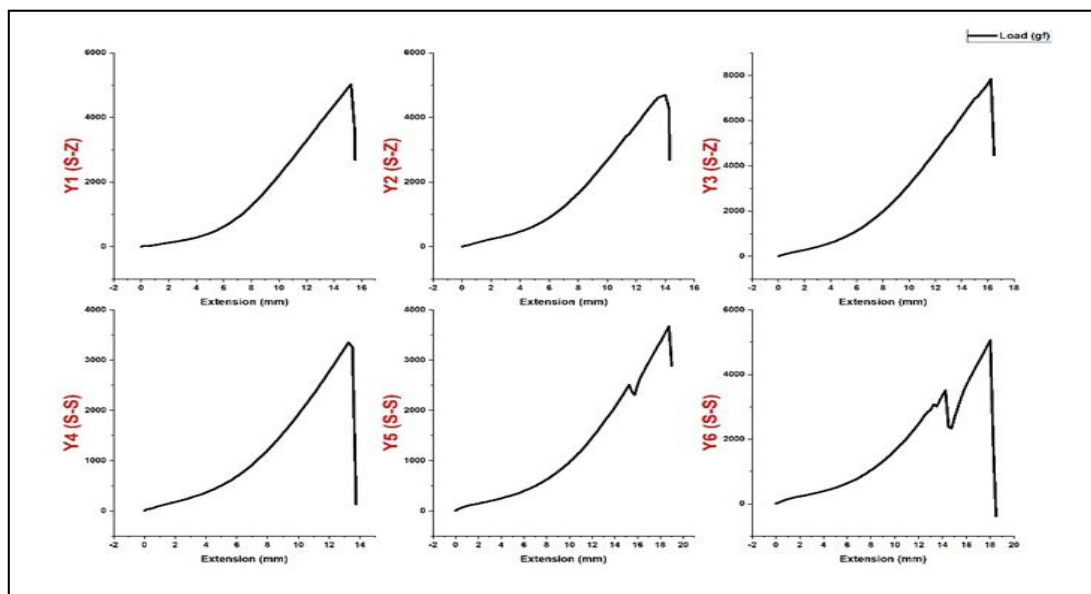


Figure 5. Tensile strength of SS core hybrid yarns

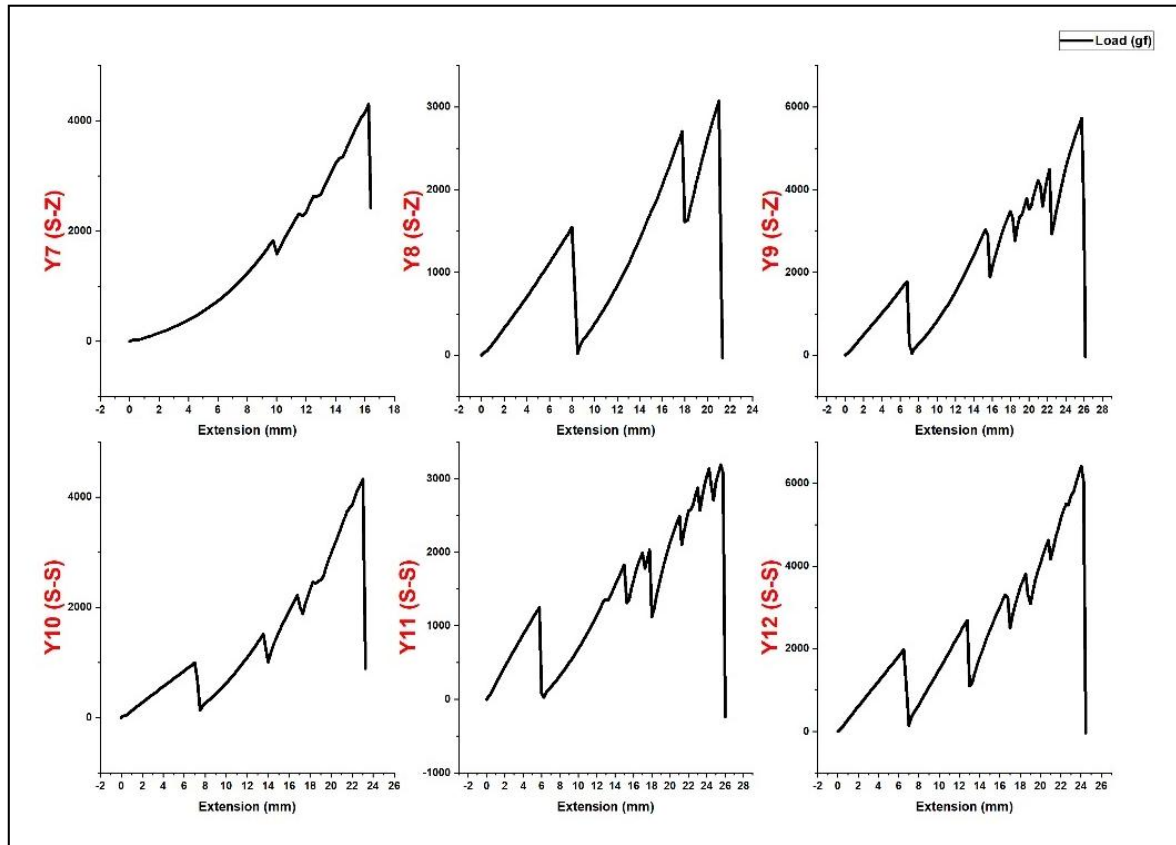


Figure 6. Tensile strength of glass core hybrid yarns

Table 3. Breaking extension of component yarns of final hybrid yarn

Fiber type	Tensile strength (N) ± SD	Tenacity (gf/den) ± SD	Modulus (gf/den) ± SD	Breaking extension (%) ± SD
SS- 30Micron	0.54 ± 0.01	5.16 ± 0.06	152.96 ± 14.55	18.52 ± 2.30
SS- 40Micron	1.44 ± 0.08	10.63 ± 0.54	142.17 ± 13.43	20.17 ± 5.45
SS- 50Micron	1.71 ± 0.03	9.84 ± 0.20	165.48 ± 14.96	28.05 ± 5.91
G-100D	9.22 ± 0.76	9.40 ± 0.78	318.07 ± 13.54	3.61 ± 0.35
G-200D	15.11 ± 1.23	7.71 ± 0.63	259.85 ± 9.48	3.81 ± 0.28
G-300D	18.61 ± 1.42	6.33 ± 0.48	210.90 ± 7.80	3.74 ± 0.19
HPPE 200D	59.16 ± 6.85	30.18 ± 3.10	616.30 ± 62.87	5.20 ± 0.35
HPPE 300D	68.54 ± 7.29	26.11 ± 2.76	548.38 ± 57.34	5.63 ± 0.39
HPPE 400D	91.11 ± 14.82	23.24 ± 3.36	500.60 ± 26.56	6.21 ± 0.55
PE-100D	4.41 ± 0.24	4.50 ± 0.25	58.74 ± 9.91	17.05 ± 1.78

Table 3 provides the breaking extension percentages of various component yarns used in hybrid yarns. Glass yarn exhibits a significantly lower breaking extension rate, ranging from 3% to 4%, compared to stainless steel (SS) yarn, which ranges between 18% and 28%. Polyester demonstrates a breaking extension rate (~20%) comparable to that of SS.

3.2 Evaluating the cracking phase of component yarns

In the case of glass-core hybrid yarns, the glass fibers reached their breaking extension limit at approximately 3% strain of the total yarn and failed first, while the other two components—polyester and HPPE—remained intact. Subsequently, polyester, having lower strength compared to HPPE, failed second, followed by the final failure of the HPPE yarn. The failure process was

documented using a video camera, revealing that HPPE, forming the outer layer, was the last to fail. The load-elongation and tensile strain curve in Figure 7 illustrates the sequential failure of the glass and polyester yarns, while multiple breaking peaks were observed after polyester failure. Table 2 shows that HPPE filaments ranged from 90 to 180 in number, with fiber diameters between 20 and 30 micrometers. Furthermore, Table 3 confirms that HPPE exhibited significantly higher tensile strength and tenacity compared to the other component yarns.

3.3 Energy at break measurement

The energy of break is typically calculated through the integration of the load-elongation curve. Most of universal strength testers provide the energy at break of entire hybrid yarn. For hybrid yarns exhibiting multiple cracking, it is essential to determine the breaking energy of each component yarn individually. Thus, by utilizing Figure 3 and Equation 4-7, the breaking energy of both the entire hybrid yarn and its individual component yarns can be calculated.

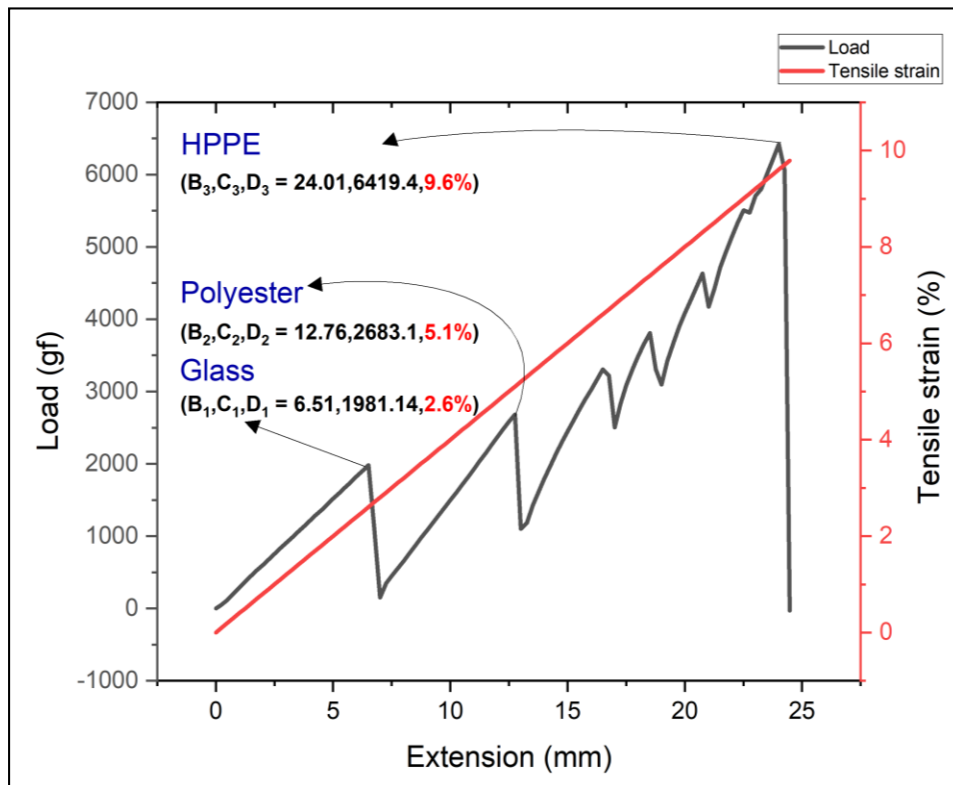


Figure 7. Layer wise yarn breaking sequence

The energy at break of Figure 4 can be calculated using the equation 4, 5, 6 and 7. From Figure 4, below data can be obtained to fit in the mentioned equations (unit of x is mm and y is gf):

$$x_1 = 6.5097, y_1 = 1981.13806, x_2 = 7.01002, y_2 = 150.67077$$

$$x_3 = 12.75991, y_3 = 2683.05185, x_4 = 13.01019, y_4 = 1101.27048$$

$$x_5 = 24.0099, y_5 = 6419.3622$$

The values of $x_1, y_1, x_2, y_2 \dots \dots$ can be obtained from the raw data of individual yarn test (Figure 4).

Breaking energy of total yarn (From equation 4)

$$\frac{1}{2}x_1 \times y_1 + \frac{1}{2} \sum_{i=1}^n (y_i + y_{i+1})(x_{i+1} - x_i)$$

$$= \frac{1}{2} \times x_1 \times y_1 + \frac{1}{2} [(y_1 + y_2)(x_2 - x_1) + (y_2 + y_3)(x_3 - x_2) + (y_3 + y_4)(x_4 - x_3) + (y_4 + y_5)(x_5 - x_4)]$$

$$= \frac{1}{2} \times 6.05097 \times 1981.13806 + \frac{1}{2} [(1981.13806 + 150.67077)(7.01002 - 6.05097) + (150.67077 + 2683.05185)(12.75991 - 7.01002) + (2683.05185 + 1101.27048)(13.01019 - 12.75991) + (1101.27048 + 6419.3622)(24.0099 - 13.01019)]$$

$$= 56998.26 \text{ gf} - \text{mm} = \frac{56998.26 \times 0.009807}{1000} \text{ joule} = \mathbf{0.559 \text{ joule}}$$

Breaking energy of glass and polyester yarn (From equation 4)

$$= \frac{1}{2} \times x_1 \times y_1 + \frac{1}{2} [(y_1 + y_2)(x_2 - x_1) + (y_2 + y_3)] = \frac{1}{2} \times 6.05097 \times 1981.13806 + \frac{1}{2} [(1981.13806 + 150.67077)(7.01002 - 6.05097) + (150.67077 + 2683.05185)(12.75991 - 7.01002)] = 15162.29811 \text{ gf} - \text{mm} = \frac{15162.29811 \times 0.009807}{1000} =$$

0.149 Joule

Breaking energy for glass yarn (From equation 5)

$$= \frac{1}{2} \times x_1 \times y_1 = \frac{1}{2} \times 6.05097 \times 1981.13806 = 5993.90 \text{ gf} - \text{mm} = 5993.90 \times \frac{0.009807}{1000} = \mathbf{0.0588 \text{ joule}}$$

The final calculation can be tabulated as below in table 4:

Breaking energy for polyester (2nd component From equation 6)

$$= \frac{1}{2} \times x_1 \times y_1 + \frac{1}{2} [(y_1 + y_2)(x_2 - x_1) + (y_2 + y_3)] - \frac{1}{2} \times x_1 \times y_1 = (0.149 - 0.0588) \text{ J} = 0.0902 \text{ J}$$

Breaking energy for HPPE (3rd component From equation 7)

$$= \frac{1}{2} \times x_1 \times y_1 + \frac{1}{2} [(y_1 + y_2)(x_2 - x_1) + (y_2 + y_3)(x_3 - x_2) + (y_3 + y_4)(x_4 - x_3) + (y_4 + y_5)(x_5 - x_4)] - \frac{1}{2} \times x_1 \times y_1 + \frac{1}{2} [(y_1 + y_2)(x_2 - x_1) + (y_2 + y_3)] = (0.559 - 0.149) \text{ J} = 0.41 \text{ J}$$

Table 4. Measuring the breaking energy of component yarns of hybrid yarn

Yarn composition	Calculated energy at break of hybrid yarn (J) (i)	Calculated breaking energy of Glass and Polyester (J) (ii)	Calculated breaking energy of glass yarn (J) (iii)	Calculated breaking energy of HPPE (J) (i-ii)	Calculated breaking energy of polyester (J) (ii-iii)
Glass core hybrid yarn (Y12)	0.559	0.149	0.0588	0.41	0.0902

3.4 Validation of the model

The breaking energy of each individual component in the hybrid yarn, as well as the overall energy at break for the hybrid yarn, can be calculated using the previously outlined procedure. Twelve different types of yarn were subjected to tensile testing, including six samples from glass-core hybrid yarns that exhibited multiple cracking. Each sample was tested ten times to obtain the final average tensile parameters. In each case, the calculated energy at break for the hybrid yarn was cross-checked against the actual energy at break values to validate the mathematical model, ensuring model accuracy.

Table 5. Calculated breaking energy of component yarns of glass core hybrid yarns

Yarn composition	Average calculated breaking energy (J)					Average actual energy (J) at break of hybrid yarn (D)	Absolute error % $(\frac{ I-I' }{I} \times 100)$	Average energy %		
	Hybrid yarn (i)	Glass and polyester (ii)	Glass (core) (iii)	HPPE (outer layer) (i-ii)	Polyester (inner layer) (ii-iii)			Glass	HPPE	Polyester
Y7 (S-Z)	0.346	0.117	0.080	0.229	0.037	0.319	8.22%	23.09%	66.27%	10.64%
Y8 (S-Z)	0.458	0.244	0.091	0.214	0.153	0.44	3.93%	19.77%	46.76%	33.47%
Y9 (S-Z)	0.580	0.163	0.049	0.416	0.114	0.560	4.39%	8.48%	71.83%	19.69%
Y10 (S-S)	0.349	0.068	0.023	0.281	0.045	0.347	5.14%	6.65%	80.41%	12.95%
Y11 (S-S)	0.449	0.129	0.046	0.320	0.083	0.431	4.01%	10.21%	71.36%	18.43%
Y12 (S-S)	0.57	0.144	0.054	0.426	0.090	0.559	3.51%	9.47%	74.78%	15.75%
						Average	4.87%	10.92%	68.57%	18.49%

Table 5 presents the breaking energy of individual component yarns during the tensile testing of glass-core hybrid yarns. The accuracy of the equation used is validated by measuring the absolute error percentage, which in most cases is less than 5%, with an average error of 4.87%. This confirms that the measurement process yields values with approximately 95% accuracy. The average breaking energy was higher for HPPE yarns and lower was observed for glass core yarn.

3.5 Surface morphology of component fibers

Figure 8 explored the fiber diameter and its surface clearly. Diameter uniformity is a highly essential factor for tensile performance of any type of yarns. The strength of any type of yarns mostly depends on its fiber quality in terms of its evenness in diameter. As all the HPPE, polyester, glass and SS yarns are man-made fibers, it shows very less variation in diameter.

4. DISCUSSIONS

4.1 Interpretation on tensile strength of hybrid yarns

The tensile behavior of hybrid yarns with stainless steel (SS) cores (Figure 5) highlights the influence of twist configuration and linear density on failure modes. The single-crack failure in S-Z twists results from counteracting torsional forces that unify stress distribution, while the S-S twist promotes multiple cracking due to increased interlayer friction and reduced compactness. Higher linear density exacerbates premature SS failure, driven by its lower elongation at break compared to HPPE and polyester. These results emphasize the critical interplay between twist configuration and the mechanical properties of individual components in determining hybrid yarn performance [28].

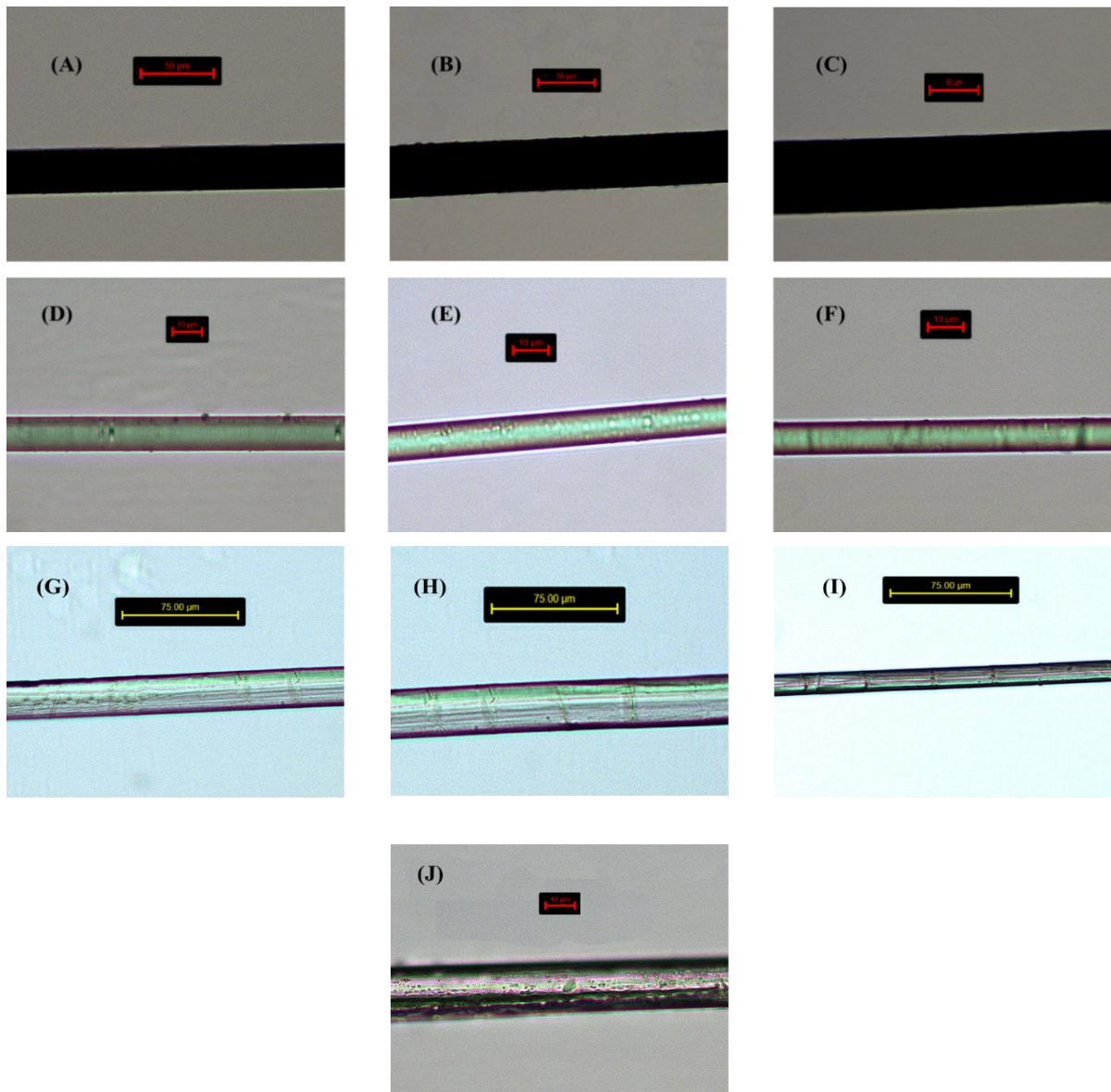


Figure 8. Fiber surface and diameter variation evidence by optical microscope (A) 30 micron SS, (B) 40 micron SS, (C) 50 micron SS, (D) 100D glass fiber, (E) 200D glass fiber, (F) 300D glass fiber, (G) 200D HPPE, (H) 300D HPPE, (I) 400D HPPE and (J) 100D polyester

In hybrid yarns with glass cores (Figure 6), twist configuration similarly impacts tensile behavior. S-S twisted yarns exhibited higher multiple-cracking tendencies due to aligned twists reducing compactness, whereas S-Z twists counteracted torsional forces, enhancing compactness and reducing cracking frequency. This aligns with prior findings that same-directed twists increase compactness and tensile strength [17]. The stepwise failure in glass-core yarns stems from the low breaking extension of glass fibers, contrasting with the more uniform failure of SS-core yarns, where multi-phase cracking is rare.

Breaking extension data in Table 3 further distinguishes the mechanical properties of component yarns. Glass yarns, with 3–4% breaking extension, exhibit brittle behavior, while SS and polyester show greater elongation capacities (~18–28% and ~20%, respectively). HPPE's low breaking extension reflects its crystalline structure and high tensile strength. These findings underline the need to optimize component selection and twist design to achieve desired mechanical properties in hybrid yarns for specific applications, such as cut-resistant textiles.

4.2 Cracking of component yarns

The failure mechanism of glass-core hybrid yarns reflects the mechanical behavior of their components in Figure 7. The early failure of glass fibers at approximately 3% strain, which is consistent with their low breaking extension percentage. Polyester, as the second component to fail, demonstrates its relatively lower tensile strength compared to HPPE, while HPPE's superior tensile properties enabled it to sustain the highest load and fail last. The multifilament structure of HPPE, as indicated by Table 2, accounts for the multiple breaking peaks observed after polyester failure, emphasizing its capacity to absorb and distribute stress effectively. Additionally, the higher tensile strength and tenacity of HPPE, confirmed in Table 3, contributed to its dominance in the final failure stage. A similar kind of result was obtained where recycled high density polyethylene yarn was twisted with cotton and the final hybrid yarn strength was increased by 36% compared to single cotton yarn [29]. The incorporation of 400 twists per meter further enhanced the yarn's performance, as the increased compactness and frictional forces between the layers provided added resistance against simultaneous failure, enabling the yarn to withstand higher loads.

4.3 Explanation of breaking energy of component yarn and model validation

Table 5 also offers insights into the contribution of each component yarn to the overall energy at break of the glass-core hybrid yarn. The outer HPPE layer contributed the largest share of breaking energy, ranging from approximately 45% to 85% with an average of 68.57%, while the inner polyester layer contributed around 10% to 34% with average of 18.49%. In most cases, the glass yarn exhibited the lowest energy (average 10.92%) contribution compared to the other yarns due to its least breaking extension rate (3.6%-3.8%) than other yarns. Moreover, glass fiber is highly brittle and less ductile in nature. For this reason, its failure in tensile load occurred in most early. In the case of S-S twisted yarns, twist is applied to the sheath layers in the same

direction. HPPE and polyester contained 400 twists per meter, giving them scope to extend a bit more than untwisted core yarn. For this, the extension % was much higher for sheath layer yarns than for core yarn. As a result, before breaking, these yarns covered a larger area under the load elongation curve and eventually experienced higher breaking energy. Untwisted core yarn directly received the tensile force and collapsed immediately after reaching its breaking extension limit [27]. The model was validated by absolute error measurement with the calculated and actual breaking energy of the ultimate hybrid yarn showing a ~95% accuracy of the model. This confirms the acceptance of this model to evaluate the breaking energy of hybrid yarn where multiple cracking takes place. Industries producing technical fabrics or composites can also adopt this model to address scenarios involving multiple cracking.

4.4 Interpretation on surface morphology of component fibers

The surface of every component fiber was found mostly smooth, and no diameter variation was evident. It confirms that there has no impact of fiber diameter irregularities on the breaking energy of the component yarns.

5. CONCLUSION

In this study, four distinct types of hybrid yarns, featuring dual sheath layers and a single core, were produced with varying yarn linear densities and twist directions. The failure patterns of the hybrid yarns, along with the energy required for their final rupture, were systematically analyzed. Notably, multiple cracking was observed in the hybrid yarns containing a glass core across all samples, while such behavior was rarely exhibited by stainless steel (SS) core yarns. Under tensile stress, the glass core yarns reached their breaking extension earlier than the other component yarns, leading to premature failure. To quantify the breaking energy of each component yarn, a mathematical model was developed based on the load-extension curves of the glass-core hybrid yarns. The model revealed that the HPPE outer layer contributed the highest average energy at break (68.67%), followed by polyester (18.49%) and glass (10.92%). The lower contribution of the glass fibers was linked to their minimal breaking extension. The developed model demonstrated an accuracy of approximately 95% in predicting the energy contributions for various compositions of glass-core yarns. Some errors were introduced due to assumptions made about the behavior of HPPE yarns during breakage, which contributed to deviations in the results. Despite this limitation, the findings provide valuable insights into the breaking energy of multicomponent materials. The assumption regarding HPPE yarn breakage remains the limitation of this study, yet the developed mathematical model holds potential for broader application. It can be extended to materials exhibiting multiple cracking behaviors, such as composites, ballistic textiles, and cut- or stab-resistant fabrics, in future research.

Acknowledgement

This research work is supported by National Technical Textile Mission (Project No: RP04561), Ministry of Textiles, India.

REFERENCES

- Hallal ,A., Elmarakbi ,A., Shaito ,A., and El-Hage ,H., (2013), *Overview of Composite Materials and their Automotive Applications*. in: Adv. Compos. Mater. Automot. Appl., Wiley, pp. 1–28.
- Puttegowda ,M., Rangappa ,S.M., Jawaid ,M., Shivanna ,P., Basavegowda ,Y., and Saba ,N., (2018), *Potential of natural/synthetic hybrid composites for aerospace applications*. in: Sustain. Compos. Aerosp. Appl., Elsevier, pp. 315–351.
- Chen ,M., Deng ,X., Guo ,R., Fu ,C., and Zhang ,J., (2022), *Tensile Experiments and Numerical Analysis of Textile-Reinforced Lightweight Engineered Cementitious Composites*. Materials. 15 (16), 5494.
- Rao ,S.V.S., Midha ,V., and Kumar ,N., (2023), *Studies on the stab resistance and ergonomic comfort behaviour of multilayer STF-treated tri-component woven fabric and HPPE laminate composite material*. Journal of the Textile Institute. 115 (4), 573–580.
- Vořechovský ,M., Li ,Y., Rypal ,R., and Chudoba ,R., (2021), *Tensile behavior of carbon textile concrete composite captured using a probabilistic multiscale multiple cracking model*. Composite Structures. 277 114624.
- Jin ,Y., Zhou ,X., Chen ,M., Zhao ,Z., Huang ,Y., Zhao ,P., et al., (2022), *High toughness 3D printed white Portland cement-based materials with glass fiber textile*. Materials Letters. 309 131381.
- Junge ,T., Brendgen ,R., Grassmann ,C., Weide ,T., and Schwarz-Pfeiffer ,A., (2023), *Development and Characterization of Hybrid, Temperature Sensing and Heating Yarns with Color Change*. Sensors. 23 (16), 7076.
- Overberg ,M., Hasan ,M.M.B., Rehra ,J., Lohninger ,E., Abdkader ,A., and Cherif ,C., (2023), *Development of multi-material hybrid yarns consisting of steel, glass and polypropylene filaments for fiber hybrid composites*. Textile Research Journal. 93 (21–22), 4865–4878.
- Hengstermann ,M., Hasan ,M., Abdkader ,A., and Cherif ,C., (2017), *Development of a new hybrid yarn construction from recycled carbon fibers (rCF) for high-performance composites. Part-II: Influence of yarn parameters on tensile properties of composites*. Textile Research Journal. 87 (13), 1655–1664.
- Park ,T.Y. and Lee ,S.G., (2017), *Properties of hybrid yarn made of paper yarn and filament yarn*. Fibers and Polymers. 18 (6), 1208–1214.
- Dalfi ,H.K., Al-Obaidi ,A., Selver ,E., Yousaf ,Z., and Potluri ,P., (2022), *Influence of yarn-hybridisation on the mechanical performance and thermal conductivity of composite laminates*. Journal of Industrial Textiles. 51 (3_suppl), 5086S-5112S.
- Beaumont ,P.W.R. and Soutis ,C., (2016), *Structural integrity of engineering composite materials: a cracking good yarn*. Philosophical Transactions of the Royal Society A: Mathematical, Physical and Engineering Sciences. 374 (2071), 20160057.
- Rypal ,R., Chudoba ,R., Scholzen ,A., and Vořechovský ,M., (2013), *Brittle matrix composites with heterogeneous reinforcement: Multi-scale model of a crack bridge with rigid matrix*. Composites Science and Technology. 89 98–109.
- Li ,Y., Chudoba ,R., Bielak ,J., and Hegger ,J., (2018), *A Modelling Framework for the Tensile Behavior of Multiple Cracking Composite*. in: pp. 418–426.
- Junaid ,K., Zyed ,M., Nonna ,A., Gaochuang ,C., and Amir ,S.L., (2024), *Tensile and cracking behaviour of crimped textile reinforced mortar (TRM) based on digital image correlation*. Construction and Building Materials. 417 135321.
- Wang ,X., Cai ,D., Silberschmidt ,V. V., Deng ,J., Tian ,H., and Zhou ,G., (2019), *Tensile properties of 3D multi-layer wrapping braided composite: Progressive damage analysis*. Composites Part B: Engineering. 176 107334.
- Ishtiaque ,S.M., Rengasamy ,R.S., Sharma ,O.P., and Das ,B.R., (2016), *Influence of fibre strength and yarn structural characteristics on tensile failure of blended spun yarns: a prediction model*. Journal of the Textile Institute. 107 (1), 127–135.
- Rengasamy ,R.S., Ishtiaque ,S.M., and Das ,B.R., (2016), *Dynamic failure behaviour of blended spun yarns during winding*. Journal of the Textile Institute. 107 (2), 242–248.
- Rebouillat ,S., Steffenino ,B., and Miret-Casas ,A., (2010), *Aramid, steel, and glass: Characterization via cut performance testing, of composite knitted fabrics and their constituent yarns, with a review of the art*. Journal of Materials Science. 45 (19), 5378–5392.
- Ceballos ,D.M., Tapp ,L.C., and Wiegand ,D.M., (2014), *Evaluation of Cut-resistant Sleeves and Possible Fiberglass Fiber Shedding at a Steel Mill*. Journal of Occupational and Environmental Hygiene. 11 (2), D28.
- Daniel (Xuedong) Li, (2019), *Choice of materials for cut protective textiles*. in: Cut Prot. Text., Woodhead Publishing India pvt ltd, pp. 165–174.
- Dessureault ,Y.S., Jolowsky ,C., Bell ,S., Spiric ,S., Molyneux ,J., Park ,J.G., et al., (2020), *Tensile performance and failure modes of continuous carbon nanotube yarns for composite applications*. Materials Science and Engineering: A. 792 (February), 139824.
- Badrul Hasan ,M.M., Nitsche ,S., Abdkader ,A., and Cherif ,C., (2019), *Influence of process parameters on the tensile properties of DREF-3000 friction spun hybrid yarns consisting of waste staple carbon fiber for thermoplastic composites*. Textile Research Journal. 89 (1), 32–42.
- Mankodi ,H. and Patel ,P., (2009), *Study The Effect Of Commingling Parameters On Glass / Polypropylene Hybrid Yarns Properties*. AUTEX Research Journal. 9 (3), 70–73.
- Schäfer ,J., Stolyarov ,O., Ali ,R., Greb ,C., Seide ,G., and Gries ,T., (2016), *Process–structure relationship of carbon/ polyphenylene sulfide commingled hybrid yarns used for thermoplastic composites*. Journal of Industrial Textiles. 45 (6), 1661–1673.
- Shahzad ,A., Ali ,Z., Ali ,U., Khaliq ,Z., Zubair ,M., Kim ,I.S., et al., (2019), *Development and characterization of conductive ring spun hybrid yarns*. The Journal of The Textile Institute. 110 (1), 141–150.
- Martín-Meizoso ,A., Martínez-Esnaola ,J.M., Scánchez ,J.M., Puente ,I., Elizalde ,R., Daniel ,A.M., et al., (1997), *Modelling the tensile fracture behaviour of the reinforcing fibre yarns in ceramic matrix composites*. Fatigue and Fracture of Engineering Materials and Structures. 20 (5), 703–716.
- Lou ,C.W., Hu ,J.-J., Lu ,P.C., and Lin ,J.-H., (2016), *Effect of twist coefficient and thermal treatment temperature on elasticity and tensile strength of wrapped yarns*. Textile Research Journal. 86 (1), 24–33.
- Suvari ,F. and Gurvardar ,H., (2024), *Revitalizing high-density polyethylene (HDPE) waste: from environmental collection to high-strength hybrid yarns*. Polymer Bulletin. 81 (15), 14011–14029.